Science & Technology Development Journal – Engineering and Technology, 4(SI3):SI117-SI131

Open Access Full Text Article

Research article

The influence of temperature to pressure and flow performance in production well

Nguyen Han Thinh[1,2], Ta Quoc Dung[1,2,*], Pham Van Hoanh[3]

ABSTRACT

Fluid temperature and pressure distribution along the borehole play a vital role in completion design, well performance, and flow assurance of the flowing fluids. Quantitative knowledge of wellbore heat transmission and pressure drop correlation is very crucial as it helps improve the accuracy of the temperature and pressure computation. It should be noted that the surrounding wellbore's components (e.g., casing, annulus fluid, cement sheath, and formation) can directly affect the fluid temperature profile due to the thermal interactions. Therefore, in this study, the primary objective is to determine the best-fit temperature model for an offshore well associated with complex borehole structures. There are three selected temperature models including Sagar et al., Alves et al., and Hasan and Kabir. In line with that, for the pressure drop model, the modified Hagedorn and Brown, which is one of the most widely used method, is also applied to the calculation process. The validity of the models has been verified by field production temperature and pressure data from the oil well SXX-P in S oil field, Cuu Long basin, Vietnam. Apart from that, sensitivity studies were also carried out to evaluate the effect of different parameters (e.g., tubing size, injection rate, and production rate) on the fluid's temperature which in turn impacts the fluid's pressure. As a result, the Hasan and Kabir appears to be the most suitable model for the temperature profile of oil well SXX-P with an average difference of 0.38%. Meanwhile, Alves et al. and Sagar et al. approaches yield a larger difference of 12% and 1.26% on average, respectively. In terms of pressure prediction, the result shows an insignificant difference which is approximately 3% with the field data by the modified Hagedorn and Brown correlation.

Key words: Fluid Temperature, Fluid Pressure, Sensitivity Studies, Oil Well Performance

[1]*Faculty of Geology and Petroleum, Ho Chi Minh City University of Technology (HCMUT), Ho Chi Minh City, Vietnam*

[2]*Vietnam National University Ho Chi Minh City, Vietnam*

[3]*Cuu Long JOC, Vietnam*

Correspondence

Ta Quoc Dung, Faculty of Geology and Petroleum, Ho Chi Minh City University of Technology (HCMUT), Ho Chi Minh City, Vietnam

Vietnam National University Ho Chi Minh City, Vietnam

Email: tqdung@hcmut.edu.vn

History

- Received: 17-5-2021
- Accepted: 27-9-2021
- Published: 04-11-2021

DOI : 10.32508/stdjet.v4iSI3.847

INTRODUCTION

Hydrocarbon production unavoidably involves significant heat exchange between the wellbore fluid and its surroundings. As hot reservoir fluids enter a wellbore and begin to travel up to the surface, they commence losing heat to the cooler surrounding sections as shown in Figure 1. Numerous studies have focused on wellbore temperature over the past several decades. Ramey (1962)[1] developed a classic model that considers fluid temperature, tubing, and casing as functions of depth and time and compared the findings with field results. Later, Shiu and Beggs (1980)[2] simplified Ramey's method by correlating for a certain coefficient in Ramey's equation that neglects the overall heat transfer calculation. Willhite (1967)[3] showed a detailed estimation for the overall heat transfer coefficient in any well completion by considering three modes of heat transfer including natural heat convection, conduction, and radiation between the flowing fluid and the cement/formation interface. For transient heat traveling away from the wellbore to an infinite formation, Hasan and Kabir (1991)[4] introduced a rigorous model that yields a superior solution than Ramey's work. Sagar et al. (1991)[5] introduced a simplified approach for predicting oil flowing temperature by correlating the term of Joule-Thomson effect and kinetic effect. Alves et al. (1992)[6] developed a unified and general temperature equation that involves fewer restrictive assumptions and derives an approximate equation for Joule-Thomson calculation. Hasan and Kabir (2009)[7] presented an analytic temperature model for treating complex well architectures. Following that, they also recommended the bottom-up calculation is more accurate than the top-down procedure.

This paper aims to investigate the best-fit temperature model of a multi-phase flowing well of deepwater production in S oil field in Cuu Long basin, Vietnam. To accomplish this, three analytical temperature models comprising Alves et al., Sagar et al., and Hasan & Kabir were applied and associated with the SXX-2P well's configuration to compute the overall heat transfer coefficient. In addition, the gas injection factor is also taken into account. Following that, the sensitivity

Cite this article : Thinh N H, Dung T Q, Hoanh P V. **The influence of temperature to pressure and flow performance in production well**. *Sci. Tech. Dev. J. – Engineering and Technology;* 4(SI3):SI117-SI131.

analysis is conducted to quantify the effects of different parameters on the wellhead temperature and temperature profiles.

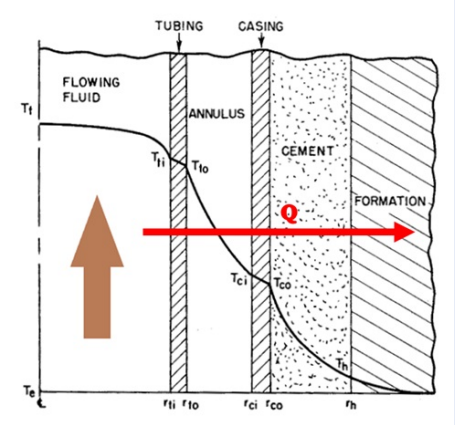

Figure 1: Wellbore heat transfer and temperature distribution[3]

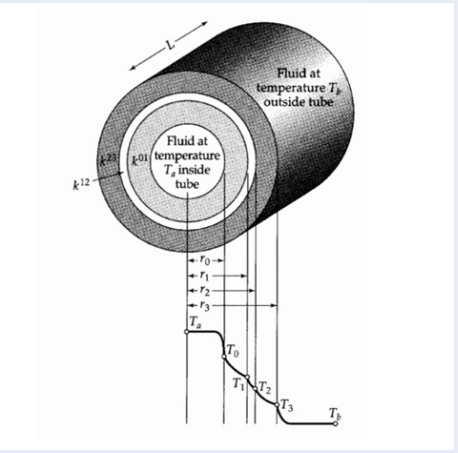

Figure 2: Heat conduction through composite cylindrical walls[8]

METHODOLOGY

Heat Transfer Mechanism

The heat transfer between hydrocarbon fluid and inside tubing wall is through forced convection. Aside from that, heat flow through the tubing wall, casing wall, and the cement sheath occurs by conduction. The annulus between the casing and tubing is often filled with completion fluids. Both radiation and natural convection occur inside the annulus. The following subsections will reveal the details of each heat loss mechanism from fluid to surrounding formation based on the work of Willhite (1967)[3].

Conductive Heat Transfer

Heat transfer resulting from conduction can be described by Fourier's equation in radial coordinates[8]. The illustration of heat transfer by conduction is in Figure 2:

$$Q = -2\pi r \triangle L k \frac{\partial T}{\partial r} \tag{1}$$

By taking integration of (1), yielding:

$$Q = \frac{2\pi k \left(T_i - T_o\right) \triangle L}{\ln\left(\frac{r_o}{r_i}\right)} \tag{2}$$

Because of the high thermal conductivity and relatively small radial distance between flowing fluids and the borehole wall, heat transfer in the following walls usually considered as steady-state:

- **Tubing wall:**

$$Q = \frac{2\pi k_t \left(T_{ti} - T_{to}\right) \triangle L}{\ln\left(\frac{r_{to}}{r_{ti}}\right)} \tag{3}$$

- **Casing wall:**

$$Q = \frac{2\pi k_{ca} \left(T_{ci} - T_{co}\right) \triangle L}{\ln\left(\frac{r_{co}}{r_{ci}}\right)} \tag{4}$$

- **Cement sheath:**

$$Q = \frac{2\pi k_{cement} \left(T_{co} - T_h\right) \triangle L}{\ln\left(\frac{r_h}{r_{co}}\right)} \tag{5}$$

Heat transfer into the surrounding rock is also by heat conduction, but it is a transient process[9]. As the volume of rock is large and can be considered as infinity, there is a large time element and steady-state conditions can often take months or years to be established. The transient radial-heat-conduction equation is expressed as:

$$Q = \frac{2\pi k_e \left(T_h - T_e\right) \triangle L}{f\left(t\right)} \tag{6}$$

Function of dimensionless time can be determined by Hasan and Kabir[4]:

$$f\left(t\right) = 1.1281\sqrt{t_D}\left[1 - 0.3\sqrt{t_D}\right) \quad for\ t_D \leq 0.5 \tag{7}$$

$$f\left(t\right) = \left[0.4063 + 0.5\ln\left(t_D\right)\right]\left[1 + \frac{0.6}{t_D}\right] \quad for\ t_D > 0.5 \tag{8}$$

Convective and Radiative Heat Transfer

- **Annulus Fluid**

Radial heat by natural convection and radiation of annulus fluid is expressed as:

$$Q = 2\pi r_{ci}\left(h_{c,an} + h_{r,an}\right)\left(T_{to} - T_{ci}\right)\triangle L \tag{9}$$

The recommended correlation for approximating convective heat coefficient in the annulus is given by Dropkin and Sommerscales[10]. Their proposed formulation is expressed as:

$$h_{c,an} = \frac{0.049\left(Gr\,Pr\right)^{\frac{1}{3}} Pr^{0.074} k_{an}}{r_{to}\ln\left(\frac{r_{ci}}{r_{to}}\right)} \tag{10}$$

The flow regime in natural convection is governed by the dimensionless Grashof number which is formulated as:

$$Gr = \frac{g\rho_{an}^2\beta\left(T_{to} - T_{ci}\right)\left(r_{ci} - r_{to}\right)^3}{\mu_{an}^2} \tag{11}$$

Prandtl number in (10) can be expressed as:

$$Pr = \frac{\mu_{an} C_{p_{an}}}{k_{an}} \tag{12}$$

The heat transfer coefficient for radiation inside the annulus can be calculated based on the Stefan-Boltzmann law[9] for a concentric annulus:

$$h_{r,an} = \frac{\sigma\left(T_{to}^2 + T_{ci}^2\right)\left(T_{to} + T_{ci}\right)}{\frac{1}{\varepsilon_{to}} + \frac{r_{to}}{r_{ci}}\left(\frac{1}{\varepsilon_{to}} - 1\right)} \tag{13}$$

The unit of temperature in (13) is in Rankine.

- **Tubing Fluid**

The radial heat by forced convection of tubing is expressed as:

$$Q = 2\pi r_{ti} h_{c,f}\left(T_f - T_{ti}\right)\triangle L \tag{14}$$

$h_{c,f}$ can be calculated by following mathematical forms:

$$h_{c,f} = \frac{k_f}{2r_{ti}} Nu \tag{15}$$

$$Nu = 0.023\left(Re\right)^{0.8}\left(Pr\right)^{\frac{1}{3}} \tag{16}$$

The Prandtl number, Pr, can be obtained by replacing the corresponding properties of tubing fluid in (12).

Overall Heat Transfer Coefficient

Radial heat transfer occurs between the wellbore fluid and the formation, overcoming various resistances in Figure 1 can be expressed[11] as:

$$Q = 2\pi r_{to} U_{to}\left(T_f - T_h\right)\triangle L \tag{17}$$

As stated earlier, due to the small radial distance between flowing fluids and the borehole wall, heat transfer is usually considered steady-state. This leads to the heat flowing through each of the elements in Figure 1 is equalized. By this analysis, the combination of (3), (4), (5), (9), and (14) generates an overall heat transfer equation:

$$U_{to} = r_{to}^{-1}\left[\frac{1}{r_{ti}h_{c,f}} + \frac{\ln\left(\frac{r_{to}}{r_{ti}}\right)}{k_t} + \frac{1}{r_{ci}\left(h_{c,an} + h_{r,an}\right)} + \frac{\ln\left(\frac{r_{co}}{r_{ci}}\right)}{k_c} + \frac{\ln\left(\frac{r_h}{r_{co}}\right)}{k_{cement}}\right]^{-1} \tag{18}$$

Some acceptable assumptions that can simplify (18). The fluid heat transfer coefficient is so high that T_f may be equal to T_{ti}. Apart from that, the high value of conductivity of metals, coupled with relatively thin tubing and casing wall, allow neglecting the resistances of these elements. Therefore, (18) can be degenerated as:

$$U_{to} = r_{to}^{-1}\left[\frac{1}{r_{ci}\left(h_{c,an} + h_{r,an}\right)} + \frac{\ln\left(\frac{r_h}{r_{co}}\right)}{k_{cement}}\right]^{-1} \tag{19}$$

Temperature Model

In this section, the analytical solution for the temperature model is presented by Alves et al., Hasan & Kabir, and Sagar et al. The mechanism of the 3 development models is the same for the temperature equation, but their expressions and assumptions are different.

General Development Model of Alves et al., Hasan & Kabir, and Sagar et al.

The derived equation of temperature profile is based on the principles of conservation of mass, momentum, and energy balance to a differential control volume of a pipe. For convenience, the proposed temperature model is expressed by Alves et al.[6]:

$$\frac{dT_f}{dL} = \frac{\left(T_f - T_e\right)}{A} - \frac{g\cos\left(\theta\right)}{C_P g_c J} - \phi \tag{20}$$

And the lumped parameter in (20) can be expressed as:

$$\phi = \frac{v}{C_P J}\frac{dv}{dL} - \eta\frac{dP}{dL} \tag{21}$$

T_e is the surrounding formation or earth temperature and can be estimated as:

$$T_e = T_{e_{bh}} - \triangle L\cos(\theta) \tag{22}$$

The difference between these methods is:
A is the relaxation distance and can be obtained by expression of Alves et al.[6]:

$$A = \frac{w_{C_p}}{2\pi r_{to}\left[U_{to} + \frac{r_{to}^{-1}k_e}{f(t)}\right]} \tag{23}$$

A is the relaxation distance and can be obtained by expression of Hasan and Kabir[7]:

$$A = \frac{f(t)\,r_{to}U_{to} + k_e}{2\pi r_{to}U_{to}k_e} \tag{24}$$

The relaxation distance (A) expression of Sagar et al.[5] is the same Hasan and Kabir. However, the heat transfer is away from the inner surface area, which means the parameter r_{to} is replaced by r_{ti}. In addition, they developed the correlation for ϕ which they called F_C:

$$\begin{aligned} F_c = \phi = &-2.978\times10^{-3} + 1.006\times10^{-6}P_{wh} \\ &+1.906\times10^{-4}w_t - 1.047\times10^{-6}R_{gL} \\ &+3.229\times10^{-5}API + 4.009\times10^{-3}\gamma_g \\ &-0.3551g_G \end{aligned} \tag{25}$$

It is important to note that if the total mass flow rate w_t is larger than 5 lb/sec the value of F_c very close to zero[5].

Pressure Model

When the fluid of oil flows through the tubing from the bottom hole to the surface, it is hard to keep the pressure above the bubble point pressure. Hence, the flowing fluid will be in two or more phases. As this circumstance happens, the flow behavior is much more complicated comparing to single-phase flow. The phases tend to separate because of differences in density. Expansion of highly compressible gas with decreasing pressure increases the in-situ volumetric flow rate of the gas. The general pressure-gradient equation for the flow in a pipe is expressed as:

$$\left(\frac{dP}{dL}\right)_{total} = \left(\frac{dP}{dL}\right)_{fri} + \left(\frac{dP}{dL}\right)_{ele} + \left(\frac{dP}{dL}\right)_{acc} \tag{26}$$

Modified Hagedorn and Brown Development Model

The modified Hagedorn and Brown method (mH-B) is an empirical two-phase flow correlation based on the original work of Hagedorn and Brown (1965)[12]. The heart of the Hagedorn and Brown method is a correlation for liquid holdup; the modifications of the original method include using the no-slip holdup when the original empirical correlation predicts a liquid holdup value less than the no-slip holdup and the use of the Griffith correlation (Griffith and Wallis, 1961) for the bubble flow regime[12].
The form of the mechanical energy balance equation used in the Hagedorn-Brown correlation in the oilfield unit is:

$$144\frac{dP}{dL} = \bar{\rho} + \frac{f\dot{w}^2}{\left(7.413\times10^{10}d^5\right)\rho_L H_L^2} \tag{28}$$

Nodal Analysis

Nodal analysis, which is defined as a system approach to oil and gas well optimization, is used to rigorously inspect a complete producing system[13]. Every component in a producing well or all wells in a producing system can be optimized to achieve the expected flow rate.
In order to solve the total system problem, nodes are placed at each segment. The portion is defined by different equations or correlations.
All present components beginning with the static reservoir pressure and ending with the separator are analyzed. Figure 3 shows an oil and gas production system with different nodes in the red circle and pressure loss estimation for each component. The focus of this study is only on wellbore nodal analysis, which combines reservoir inflow with wellbore lift capability by intersecting the IPR (inflow performance relationship) and TPR (tubing performance relationship) curves on a pressure and production rate plot to predict operating flow rate. Following that, the sensitivity evaluation is carried out to optimize the production or to find any other possible problems with the changes of different parameters.

Inflow Performance

The IPR visualizes the relationship between the well's producing bottom-hole pressures and its corresponding production rates under a given reservoir condition.

Tubing Performance

The TPR defines as the performance of the flowing fluid through the tubing in the borehole by generating the plot of bottom-hole pressure and corresponding flow rate. To construct the performance of flowing fluid through the wellbore, it is essential to determine the changes of pressure and temperature for a stabilized flow rate. As these values change, the independent properties of the flow will vary significantly. Therefore, to handle this issue, the black oil model appears to be a very important tool.

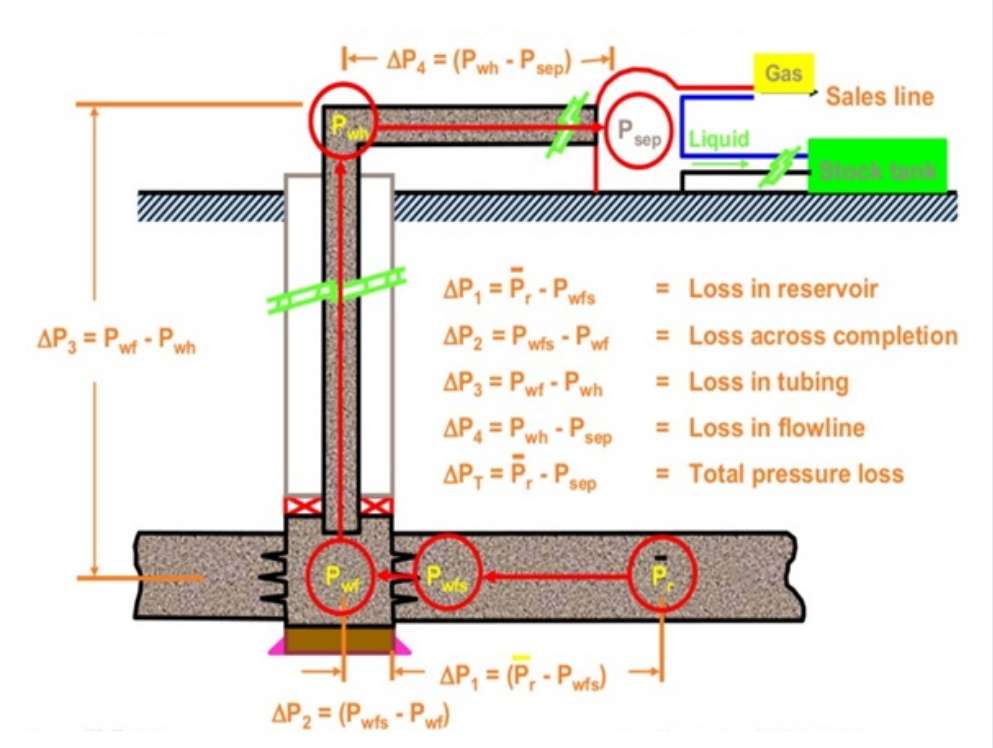

Figure 3: Common nodes at different locations in the system [14]

RESULT AND DISCUSSION

In this section, the predicted model was compared to the actual field data in oil well SXX-2P in S oil field to show the reliability of the proposed approach. Aside from that, the sensitivity studies will be carried out to analyze the changes of parameters that can evaluate oil well performance.

Well Data Acquisition and Analysis

Well Deviation Survey

Before embarking on the simulation of field cases and sensitivity analysis, the data acquisition and analysis is a crucially initial step.

The side view of the oil well SXX-2P is illustrated in Figure 4. It shows that from the depth of 0 to 1800 ft the well is a perfect vertical. However, as the well was continuously drilled down to nearly 11000 ftTVD, the inclination angle varies slightly to moderately in different degrees. The well is about to be significantly deviated as moving forward in a range of 12000 ftTVD to 14000 ftTVD.

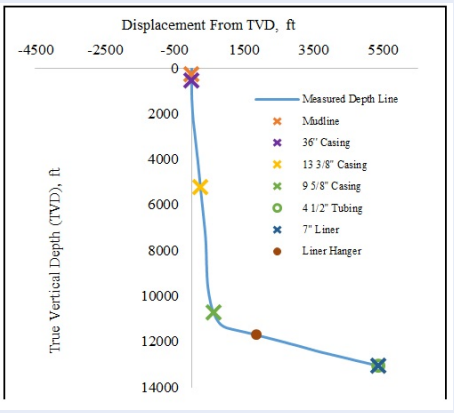

Figure 4: Oil well SXX-2P schematic

Well Test Data

From the well test data information in Table 1, it is clear that the well flow is supported by gas lift at the depth of 1995 mMD (6545.28 ftMD). It also indicates the gas injection rate which is about 3.5 MMscf/day. The model of pressure, thus, must be taken into account the gas lift for matching with the field data. The water cut, on the other hand, is so high that needs to be carefully considered a suitable correlation for the flowing pressure in the inflow and tubing flow performance. In the sensitivity studies section, the effect of

Table 1: Well test data of oil well SXX-2P

Well Test Information		
Wellhead pressure	304	psig
Wellhead temperature	240.8	^{o}F
Water cut	0.85	
Liquid rate	4725	bbl/day
Gas injection rate	3.5	MMscf/day
Gas injection depth	6545.28	ft
Gauge depth (MD)	10898.95	ft
Gauge temperature	296.24	oF
Gauge pressure	2946	psig

gas injection and injection depth is evaluated to find other possible selections.

Borehole Schematic for Calculating Overall Heat Transfer

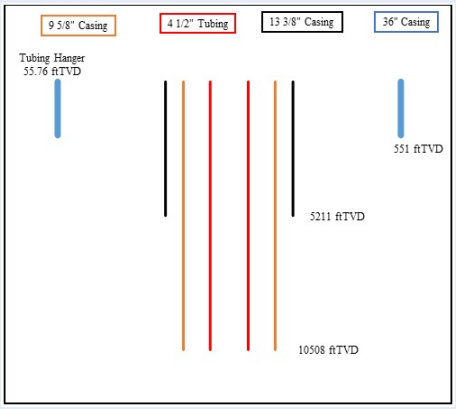

Figure 5: Modeling segment of well SXX-2P

Figure 5 shows a general wellbore architecture from the tubing hanger to the 9 5/8" casing shoe. This segment is selected to model because the data of temperature and pressure profile are provided.

Pressure and Temperature Model

Coupling algorithm: two levels of sophistication can be employed when coupling the heat balance and mechanical energy balance equations to calculate pressure and temperature changes simultaneously. Convergence on both pressure and temperature in a given pipe length increment requires a double-iterative procedure. The general workflow to obtain the pressure and temperature at certain segment can be executed by applying the flowchart in Figure 6.

The overall heat transfer coefficient can be calculated through the workflow in Figure 7. In particular, this flowchart shows a procedure of using series of equations in the appendix section for estimating the overall heat transfer coefficient.

The error was calculated by (29) to find the difference between the predicted value from the proposed model and the measured value collected from the well.

$$Error = \frac{|Predicted\ Value - Measured\ Value|}{Measured\ Value} \quad (29)$$

The plot of pressure gradient for oil well SXX-2P is demonstrated in Figure 8. It shows a plot of pressure versus depth. The measured pressure is given from a depth of 11180 ftMD up to 55.8 ftMD of a tubing hanger. It is should be noted that the depth of the gas lift injection is about 6550 ftMD with 3.5 MMscf/day of gas rate and the model is developed from the bottom node.

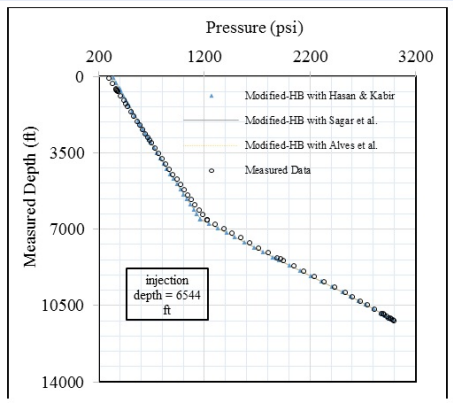

Figure 8: Predicted Pressure with Measured Data

Table 2: Borehole survey of oil well SXX-2P

Wellbore Component	Drilling depth (ftTVD)	Hole size (in)
Mudline	255	36
36-in conductor shoe	551	36
13 3/8-in casing shoe	5211	16
9 5/8-in casing shoe	10508	12.25
4 1/2-in tubing shoe	10508	12.25

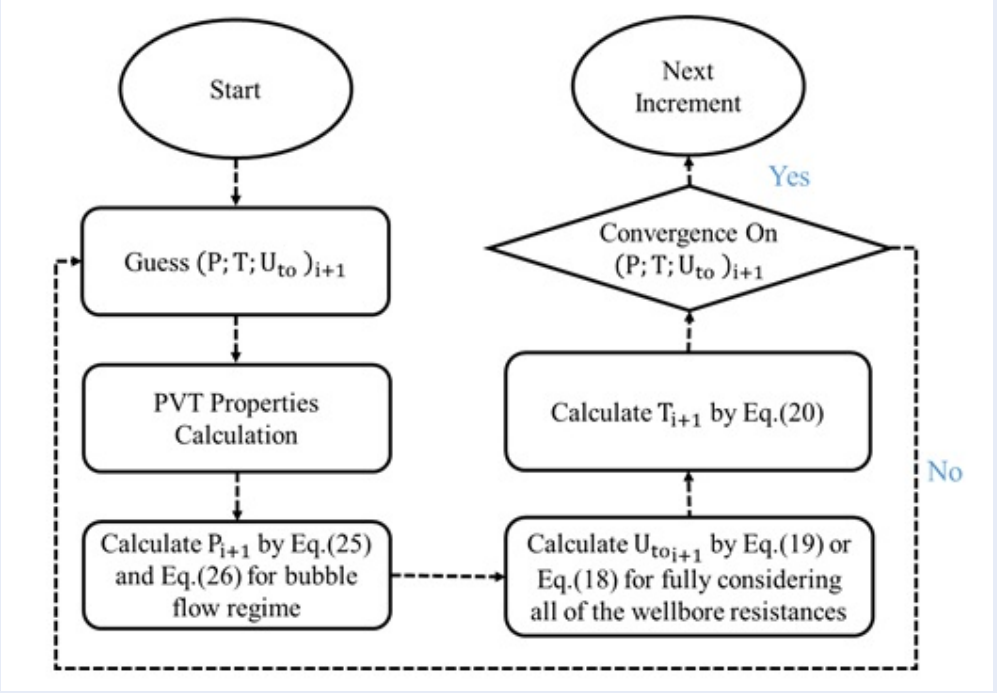

Figure 6: Simplified workflow for calculating P, T

The plot of temperature gradient for oil well SXX-2P is provided in Figure 9. It shows a difference in applying the three rigorous temperature models, the simple linear interpolation method, and measured temperature. It is evident that the temperature profiles of Hasan & Kabir and Sagar et al. generally matched with the measured data whereas the usually used linear interpolation and the Alves et al. yield a significant error. Looking at Figure 9, there is a high possibility that Hasan & Kabir is the best-fit model for oil well SXX-2P temperature profile.

More details of error or difference between the predicted value and the measured data are presented by Figure 10 and Figure 11 as follows. Besides, it must be recognized that the negative value of difference indicates the underestimation of the model to the measurement, and conversely, the positive difference

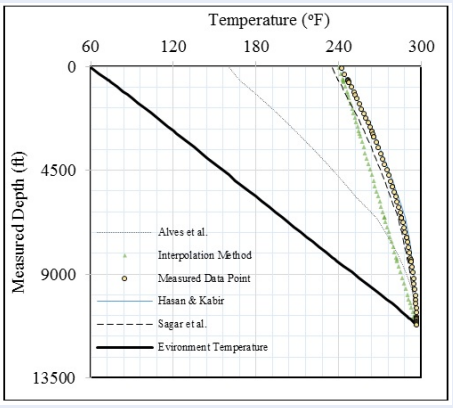

Figure 9: Temperature prediction with measured data

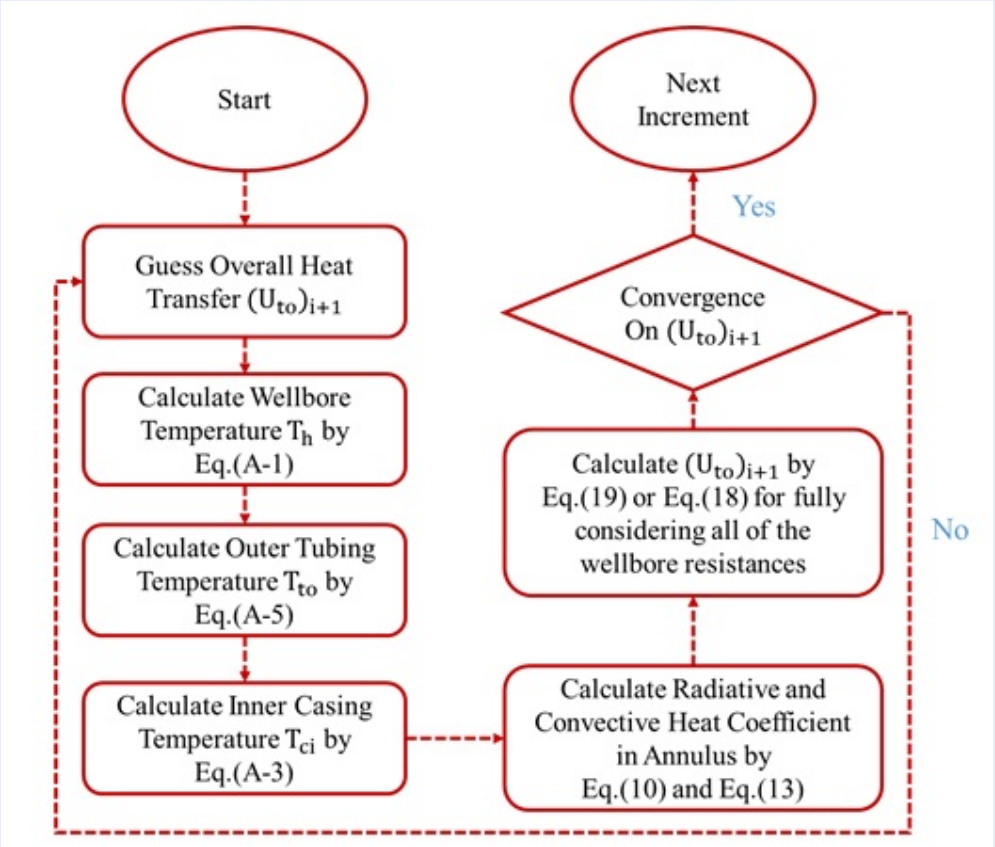

Figure 7: Solving process of calculating overall heat transfer coefficient

means overpredicted value.

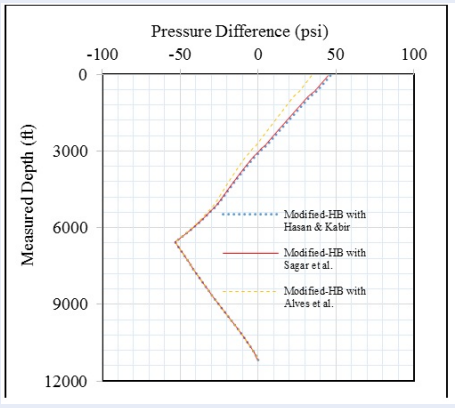

Figure 10: Pressure Difference with Measured Data

Through Figure 10, the pressure prediction by modified HB generally gives a very good agreement with the measured data when coupling with three temperature models. Particularly, the difference ranges from -50 psi to 50 psi. It can be noted that the modified HB and Alves et al. combination yields less error in pressure prediction. This can be explained that the predicted temperature is smaller than the Hasan & Kabir, and Sagar et al. models leading to the viscosity is higher and as the result, the pressure loss is larger.

The difference between the measured and predicted value of temperature is plotted in Figure 11. Overall, Sagar et al. and Hasan & Kabir temperature models yield an excellent match with the absolute difference ranging from 0 ^{o}F to 6 ^{o}F and from 0 ^{o}F to 3 ^{o}F, respectively. Meanwhile, a considerable underestimation is observed from the model of Alves et al. In particular, the Alves et al. model gives absolute difference ranging from 0 ^{o}F to 81 ^{o}F.

Table 3 shows an average difference in temperature models with measured data by percentage when coupling with modified-HB pressure correlation. The results show that Hasan & Kabir is the best-fit temperature model for the SXX-P2 oil well.

The overall heat transfer coefficient is estimated based on the well SXX-2P's architecture given in Figure 5

Table 3: Average difference of temperature and pressure with measured data

Temperature Model	Average T Difference (%)	Average P Difference (%)
Alves et al.	12	2.56
Hasan & Kabir	0.38	3
Sagar et al.	1.26	3

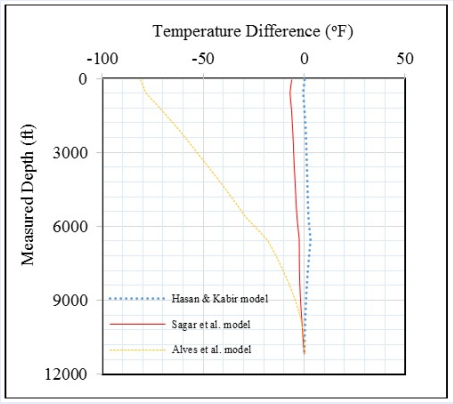

Figure 11: Temperature difference with measured data

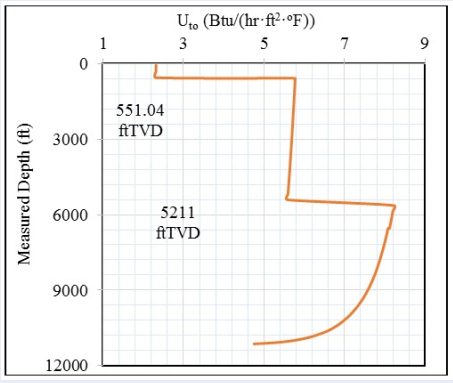

Figure 12: Overall heat transfer along the wellbore depth

and borehole size in Table 2. Particularly, there are 3 sections for analysis of the wellbore resistances.

Section 1: From 55.76 ftTVD to 551 ftTVD, cement is filled between 36" and 13 3/8" casing, 13 3/8" and 9 5/8" casing. The annulus fluid is filled between 9 5/8" casing and 4 1/2" tubing. The thickness of cement is largest leading to the smallest overall heat transfer coefficient.

Section 2: From 551 ftTVD to 5211 ftTVD, the gap between 16" borehole size and 13 3/8" casing filled with cement. The 13 3/8" and 9 5/8" casing is also filled with cement. Therefore, the thickness of cement reduces leading to the increase of overall heat transfer coefficient.

Section 3: From the 5211 ftTVD to the end of tubing shoe in modeling segment. Borehole size is 12.25-in leading to cement thickness gets smaller, the annulus convective and radiative effects are dominant.

The overall heat transfer coefficient along the depth of the wellbore is depicted in Figure 12. Generally, as the fluid raises upward to the surface, the resistance of the outer components becomes larger leading to the overall heat transfer to the surrounding components is smaller.

Sensitivity Analysis

This section is conducted by keeping in mind that the proposed approach is already matched with the measured data with accepted error. In case, a significant error happens, the calibration is made with appropriation. For instance, the heat convection in the annulus is estimated by correlation therefore, we can adjust the value by 25% of that calculation. This case was carried out by Hasan and Kabir[9] because according to their calculation, the value of convective heat coefficient is usually higher than the expected value.

In the following sections, Hasan & Kabir temperature model is used in the sensitivity analysis with modified Hagedorn & Brown pressure correlation.

Effect of Flow Rate

The effect of various flow rates on the wellhead temperature and pressure is illustrated in Figure 13. The temperature axis is on the right-hand side and the pressure axis is on the left-hand side. It should be noted that the fixed node is located at the bottom hole, thus, changing the production rate leads to the variation of pressure and temperature in the wellhead.

Overall, due to the decrease of production rate from 4725 to 500 stb/day, the wellhead pressure increases from 340 to 741 psi. In contrast, the corresponding temperature shows a sharp decline from 241 to 138.6 ^{o}F.

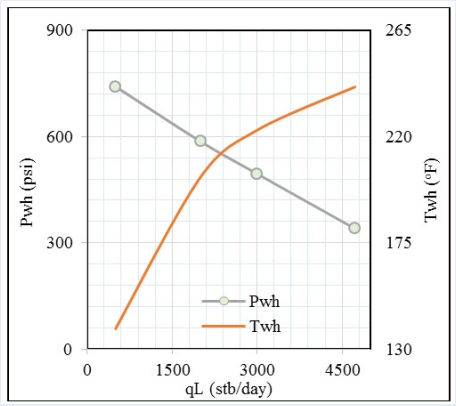

Figure 13: Effect of flow rate changes to wellhead temperature and pressure of oil well SXX-2P

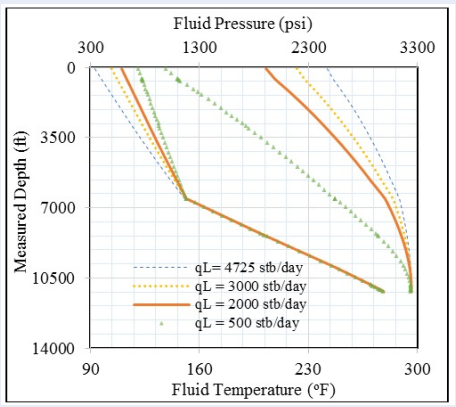

Figure 14: Effect of flow rate changes to fluid temperature and pressure of oil well SXX-2P

Figure 14 shows a more general temperature and pressure of fluid plot as the production rate declines. The fluid pressure is at the top horizontal and the fluid temperature axis is at the bottom. Overall, the fluid temperature decreases with increasing pressure under the reduction of production rate.

Effect of Tubing Size

It should be noted that the change of tubing size will lead to the variation of the operating production. Thus, to make a thorough analysis, the study is conducted under the changes of tubing size at fixed operating production and various operating production.

Fixed Operating Production

This evaluation is carried out by putting a node at the bottom of the borehole to observe the change of pressure and temperature in the wellhead. The operating production rate is 4725 stb/day.

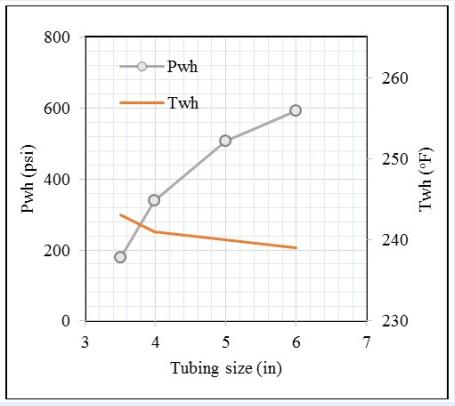

Figure 15: Effect of tubing size changes on wellhead temperature and pressure

The effect of different tubing sizes on the wellhead is demonstrated in Figure 15. By making some adjustments in tubing size, the variation of pressure and temperature at the wellhead occurs. Generally, as the tubing size gets larger, the wellhead pressure increases significantly whereas the wellhead temperature gains a slight decrease. In particular, tubing size increases from 3.5 to 6 in, the recorded wellhead temperature decreases from 243 to 239 ^{o}F. The pressure, however, gains a fairly large increase from 179 to 592 psi.

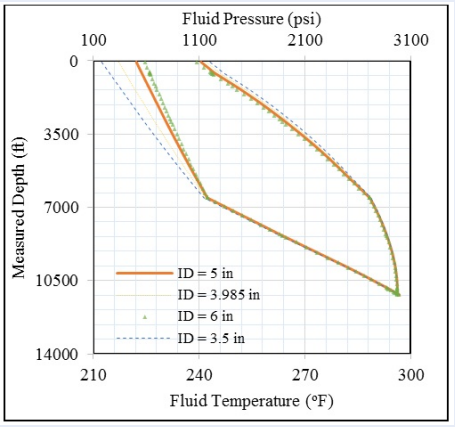

Figure 16: Effect of tubing size changes on fluid temperature along the wellbore

Figure 16 shows a more general fluid temperature and pressure profiles along the borehole of oil well SXX-2P under various tubing sizes. In short, this illustration shows that the tubing size has a great influence on the fluid pressure and a minor impact on the fluid temperature at the fixed production rate. As the tubing

size enlarges, the heat loss to the radial distance will expand. As the result, the fluid temperature will decrease.

Various Operating Production

By enlarging the tubing size, the flow rate can increase at the operating point. This point indicates the actual production will be produced at the surface. The node in these cases is fixed and set at 304 psi at the wellhead location.

Figure 17 shows that when combining TPR and IPR curve, the produced liquid rate is about 4810 stb/day at the bottom-hole flowing pressure of 2941 psi.

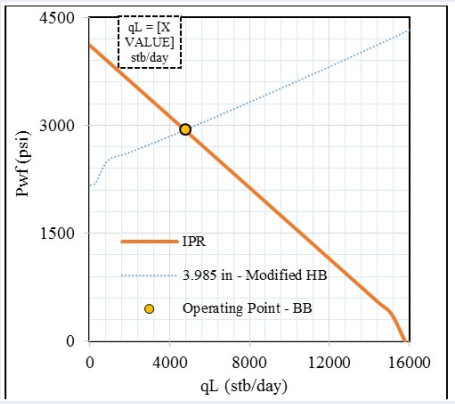

Figure 17: Well deliverability of oil well SXX-2P

Table 4 confirms that the prediction by the proposed model provides an excellent match with actual well test data of oil well SXX-2P. The percentage of error is very small for operating point comparison. In particular, the predicted production rate gives a difference of 1.8 %. The predicted wellhead temperature also matches with wellhead data with 0.083 percentage of difference.

Figure 18 shows the illustration of various operating production with corresponding tubing diameters of oil well SXX-2P analysis.

In other cases, as we replace various tubing sizes of 3.5, 5, 6 in instead, the production changes considerably. Particularly, as increasing tubing sizes, the production at the node will increase with the reduction of bottom-hole pressure. The change of tubing size is limited because of the liner production size in Figure 4.

Table 5 shows that by changing the tubing sizes the produced fluid will vary significantly. This leads to an increase of wellhead temperature and in turn, the recorded pressure at the bottom decreases.

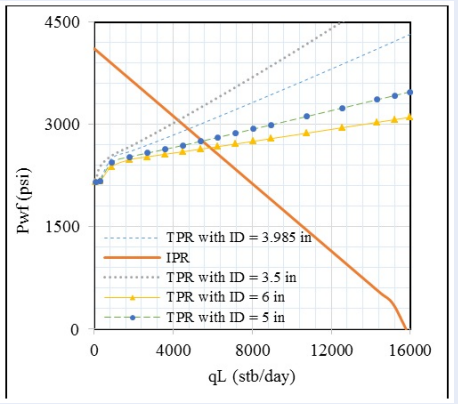

Figure 18: Oil well SXX-2P deliverability plot for various tubing sizes

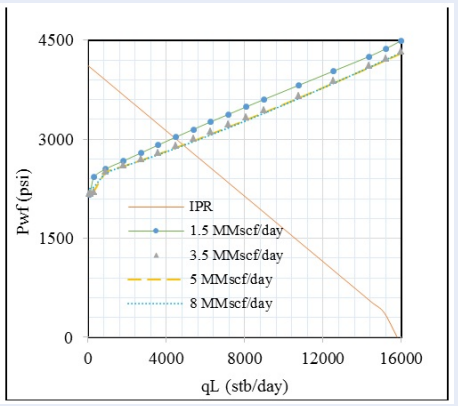

Figure 19: Oil well SXX-2P for various gas injection rate

Effect of Gas Injection Rate

The effect of various gas rate injections on IPR and TPR combination plots is shown in Figure 19. It is important to note that the given injection rate in the field is 3.5 MMscf/day, however, to find the more possible gas injection amount, the sensitivity is carried out by varying the rate of gas injection. Figure 19 indicates that the rate of 1.5 MMscf/day gives a poor value of production rate. By rising the amount of gas injection rate from 3.5 to 8 MMscf/day, the operating production is accelerated.

Looking at the performance curve Figure 20 and Table 6, it is clear that the maximum oil production of 4915 stb/day occurs for gas lift rate of approximately 8 MMscf/day.

In case the gas rate of injection is operated at 10 MMscf/day, the production starts to reduce. This is due to the increase of gas injection will increase friction

Table 4: Comparison between the predicted and measured operating point

ID = 3.985 in	Calculated	Measured	% Error
qL (stb/d)	4810	4725	1.8
Pwf (psi)	2941	2964	0.776
Twh (^{o}F)	241	240.8	0.083

Table 5: Solution node at different tubing sizes

ID (in)	qL (stb/d)	Pwf (psi)	Twh (^{o}F)
3.5	4250	3070	238
5	5515	2763	245
6	5920	2662	246.5

Table 6: Solution node at different injection rate

ID (in)	qL (stb/d)	Pwf (psi)	Twh (^{o}F)
1.5	4411	3023	238
3.5 (data)	4810	2941	241
5	4845	2915	242
8	4915	2910	244
10	4850	2915	243

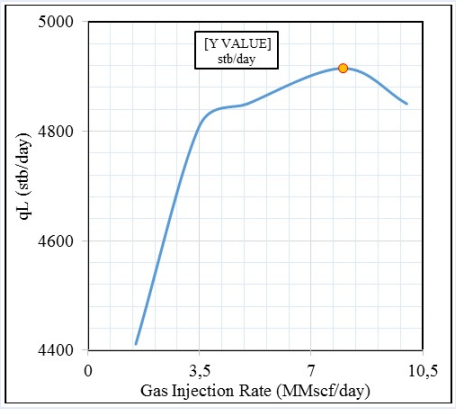

Figure 20: Effect of gas rate injection on the production of oil well SXX-2P

component more than it will decrease gravity component. After this stage, any increase in the gas injection will decrease production rates. Thus the performance curve will go up and then come down as shown in Figure 20. It should be noted that increasing the injected gas rate does not show any positive effects on oil well SXX-2P. This is due to the produced rate is just about 100 stb/day if we scale up the gas lift injection to 8 MMscf/day from the data field 3.5 MMscf/day.

CONCLUSION

1. In this study, the detailed solving process for computing the temperature and overall heat transfer profiles along the complex borehole layout is presented. It can be applied to any complex wellbore structure by modifying the thermal resistances in overall heat transfer coefficient.
2. The proposed approaches are applied to the oil well SXX-2P. Comparison of three different temperature models and measured data indicates that Hasan & Kabir is the best-fit temperature model with an average difference of 0.38%. In line with that, modified Hagedorn & Brown shows 3% and 1% difference in predicting pressure transverse and solution node of the oil well SXX-2P, respectively.
3. The sensitivity analysis is conducted to find the effects of tubing size, production rate and injection gas rate on temperature and pressure along the wellbore in the location of the node at the wellhead and bottom-hole of the well. Based

on the sensitivity analysis, the following conclusions are listed below:

- **The flow rate changes** yield a great influence in both temperature and pressure. By reducing the rate from 4725 to 500 stb/day the, pressure at the wellhead increases from 340 to 741 psi while the temperature gains a reduction of approximately 104 ^{o}F from 241 ^{o}F.
- **The tubing size** has a huge impact on pressure profile whereas affecting the temperature slightly. For the fixed production rate, by increasing the tubing size from 3.5 to 6 in, the pressure in the wellhead increases from 180 to 600 psi. However, the wellhead temperature only gains a slight decrease from 243 to 239 ^{o}F. In case of the various operating production rates, the changes of tubing diameter generate a larger influence in temperature and pressure. In particular, by altering the size of tubing from 3.5 to 6 in, the production rate accelerates from 4250 to 5920 stb/day. As the results, the wellhead temperature increase from 238 to 246.5 ^{o}F meanwhile the bottom-hole pressure declines from 3070 to 2662 psi.
- **As gas injection rate** increases in the range of 1.5 to 3.5 MMscf/day (field data), the amount of produced liquid is nearly 400 stb/day. However, if we continue to push more the injected gas rate to 8 MMscf/day, the gained production is only 70 stb/day. This implies the 3.5 MMscf/day of gas injection in operating field condition of oil well SXX-2P is still appropriate. In case of 10 MMscf/day, the produced started to decline. In terms of temperature, the influence is minor as recorded from Table 6.

ACKNOWLEDGMENT

This research is funded by Vietnam National University HoChiMinh City (VNU-HCM) under grant number **(C2021-20-39)**.

ABBREVIATIONS

IPR: inflow performance relationship
TPR: tubing performance relationship
Pwh: wellhead pressure
Pwf: bottom hole pressure
HB: Hagedorn and Brown
TVD: true vertical depth
MD: measured depth

NOMENCLATURES

$\triangle L$: length of each segment, ft
g_C: conversion factor, 32.17 lbm·ft/(lbf·sec^2)
h_C: convective heat coefficient, Btu/(hr·ft^2·^{o}F)
h_L: holdup liquid
h_R: radiative heat coefficient, Btu/(hr·ft^2·^{o}F)
t_D: dimensionless time
U_{to}: Overall heat transfer coefficient, Btu/(hr·ft^2·^{o}F)
$\bar{\rho}$: average mixture density, lb/ft^3
A: relaxation distance, ft
$C_{p:}$ Specific-heat capacity, Btu/lb·^{o}F
d: Inner tubing diameter, ft
f: Friction factor
f(t): Transient heat conduction function
g: gravitational acceleration, ft/sec^2
Gr: Grashof number
J: conversion factor for the mechanical equivalent of heat, ft·lbf/Btu
k: thermal conductivity
Nu: Nusselt number
P: pressure, psi
Pr: prandtl number
r: radial distance or radius, ft
Re: Reynold number
T: temperature, ^{o}F
v: velocity, ft/sec
w: mass rate, lb/ft^3
β: fluid thermal expansion coefficient, 1/^{o}F
ε: emissivity
η: Joule-Thomson coefficient, ^{o}F·ft^2/lbf
θ: inclination angle
σ: Stefan-Boltzmann constant, 1.731x10^{-9} Btu/(hr·ft^2·^{o}R^{-4})
ϕ: lumped parameter, ^{o}F/ft
q: flow rate, stb/day
R_{gL}: gas/liquid ratio, scf/stb
w_t: total mass flow rate, lb/sec
Q: heat flow rate, Btu/hr

SUBSCRIPTS

an: annulus
f: fluid
to: outer tubing
ci: inner casing
co: outer casing
ca: casing
t: tubing
wh: wellhead
wf: bottom hole
L: liquid
fri: friction
acc: acceleration

ele: elevation
bh: bottom hole
h, wb: borehole, wellbore

Interest of Conflict

The author pledges the topic "The Influence of Temperature to Pressure and Flow Performance in Production Well" is the research of the author. Figures and results in the report are true and no competing interest.

AUTHOR S' CONTRIBUTION

Nguyen Han Thinh: Studied theories and performed the methodology of temperature and pressure models, carried out the sensitivity studies for analyzing the effect of different parameters on the pressure, temperature and production, wrote the manuscript with the support from **Ta Quoc Dung** and **Pham Van Hoanh.** **Ta Quoc Dung, PhD.:** Management and coordination responsibility for the research activity planning and execution, made critical revision of the manuscript, gave suggestions and resources for improving the research, assessed the reliability of the research's results.

SPEC. Pham Van Hoanh: Conceived the presented idea, data acquisition, provided technical helps on the temperature and pressure issues when modeling, made analysis and interpretation of data.

APPENDIX

In this section, the expressions for calculating temperature of wellbore, casing, and tubing are derived. For steady-state heat transfer, the radial heat flow is constant for specific interval of length.

By combining (6) and (17), wellbore temperature T_h is expressed as:

$$T_h = \frac{k_e T_e + f(t)\, r_{to} U_{to} T_f}{k_e + f(t)\, r_{to} U_{to}} \tag{17}$$

After obtaining T_h, the outer casing temperature is obtained through combination of (5) and (17):

$$T_{co} = T_h + \frac{\ln\left(\frac{r_h}{r_{co}}\right)(T_f - T_h)\, U_{to} r_{to}}{k_{cement}} \tag{A-2}$$

Then calculating inner casing temperature by (4) and (17):

$$T_{ci} = T_{co} + \frac{\ln\left(\frac{r_{co}}{r_{ci}}\right)(T_f - T_h)\, U_{to} r_{to}}{k_{ca}} \tag{A-3}$$

The inner tubing calculated by (14) and (17):

$$T_{ti} = T_f - \frac{(T_f - T_h)\, U_{to} r_{to}}{r_{ti} h_{c,f}} \tag{A-4}$$

The outer tubing temperature can be obtained by (3) and (17):

$$T_{to} = T_{ti} - \frac{\ln\left(\frac{r_{to}}{r_{ti}}\right)(T_f - T_h)\, U_{to} r_{to}}{k_t} \tag{A-5}$$

REFERENCES

1. Ramey H. Wellbore heat transmission. J. Pet. Technol. 1962;p. 427–435. Available from: https://doi.org/10.2118/96-PA.
2. Shiu KC, Beggs HD. Predicting Temperatures in Flowing Oil Wells. ASME. J. Energy Resour. Technol. 1980;Available from: https://doi.org/10.1115/1.3227845.
3. Willhite G. Overall heat transfer coefficients in steam and hot water injection wells. J. Pet. Technol. 1967;p. 607–615. Available from: https://doi.org/10.2118/1449-PA.
4. Hasan AR, et al. Heat Transfer During Two-Phase Flow in Wellbores; Part I–Formation Temperature. SPE Annual Technical Conference. 1991;PMID: 1744079. Available from: https://doi.org/10.2118/22866-MS.
5. Doty SR, et al. Predicting Temperature Profiles in a Flowing Well. SPE Pro Eng. 1991;6:441–448. Available from: https://doi.org/10.2118/19702-PA.
6. Alves IN, et al. A Unified Model for Predicting Flowing Temperature Distribution in Wellbores and Pipelines. SPE Pron Eng. 1992;7:363–367. Available from: https://doi.org/10.2118/20632-PA.
7. Rashid HA, et al. A Robust Steady-State Model for Flowing-Fluid Temperature in Complex Wells. SPE Prod & Oper. 2009;24:269–276. Available from: https://doi.org/10.2118/109765-PA.
8. Bird RB, et al. Transport phenomena, New York: John Wiley & Sons, Inc. 2007;.
9. Hasan AR, et al. Fluid Flow and Heat Transfer in Wellbore, Texas: SPE, 2002;.
10. Dropldn, et al. Heat Transfer by Natural Convection in Liquids Confined by Two Parallel Plates Inclined at Various Angles With Respect to the Horizontal. J. Heat Transfer. 1965;p. 77. Available from: https://doi.org/10.1115/1.3689057.
11. Brill JP, Mukherjee HK. Multiphase Flow in Wells, Pennsylvania: Henry L. Doherty Memorial Fund of AIME, Society of Petroleum Engineers. 1999;.
12. Guo B, Lyons WC. Petroleum production engineering: a computer-assisted approach, Elsevier Science & Technology Books, 2007;.
13. Beggs. Production Optimization Using Nodal Analysis, Tulsa, Oklahoma: OGCI and Petroskills. 2003;.
14. Altam RAA. Production Optimization by Nodal Analysis. Universiti Teknologi PETRONAS, Tronoh. 2015;.

Tạp chí Phát triển Khoa học và Công nghệ – Engineering and Technology, 4(SI3):1-1

Open Access Full Text Article

Bài nghiên cứu

Ảnh hưởng của nhiệt độ lên áp suất và lưu lượng dòng chảy trong giếng khai thác

Nguyễn Hán Thịnh[1,2], Tạ Quốc Dũng[1,2,*], Phạm Văn Hoanh[3]

Use your smartphone to scan this QR code and download this article

TÓM TẮT

Sự phân bố nhiệt độ và áp suất của chất lưu dọc theo thân giếng đóng một vai trò quan trọng trong thiết kế hoàn thiện, hiệu suất khai thác và đảm bảo dòng chảy. Kiến thức định lượng về truyền nhiệt ở thân giếng và tương quan áp suất là rất quan trọng vì nó giúp cải thiện độ chính xác trong việc tính toán nhiệt độ và áp suất. Cần lưu ý rằng các thành phần xung quanh giếng (ví dụ: ống chống, dung dịch khoảng không vành xuyến, lớp xi măng và thành hệ) có thể ảnh hưởng trực tiếp đến nhiệt độ chất lưu do tương tác nhiệt. Vì thế, trong nghiên cứu này, mục tiêu chính là xác định mô hình nhiệt độ phù hợp nhất cho giếng ngoài khơi có cấu trúc giếng phức tạp. Ba mô hình nhiệt độ được lựa chọn gồm Sagar et al., Alves et al., và Hasan & Kabir. Đối với mô hình áp suất, Hagedorn & Brown cải tiến, một phương pháp được sử dụng rộng rãi cũng được áp dụng vào trong quá trình tính toán. Tính hợp lệ của các mô hình được xác minh bằng dữ liệu nhiệt độ và áp suất khai thác thực tế đo đạc từ giếng dầu SXX-P tại mỏ dầu S, bể Cửu Long, Việt Nam. Ngoài ra, các nghiên cứu về độ nhạy cũng được thực hiện để đánh giá ảnh hưởng của các thông số khác nhau (ví dụ: kích thước ống, lưu lượng bơm ép và lưu lượng khai thác) đến nhiệt độ của chất lưu, từ đó tác động lên áp suất của chất lưu. Theo kết quả kiểm tra với số liệu thực tế, mô hình nhiệt độ của Hasan & Kabir là phù hợp nhất cho giếng dầu SXX-2P với phần trăm chênh lệch trung bình là 0.38%. Trong khi phần trăm chêch lệch trung bình lớn hơn ghi nhận được từ mô hình của Alves et al. và Sagar et al. lần lượt là 12% và 1.26%. Về dự đoán áp suất bằng tương quan Hagedorn & Brown cải tiến, kết quả cho thấy sự khác biệt không đáng kể, xấp xỉ 3% với dữ liệu thực tế.

Từ khoá: Nhiệt Độ Chất Lưu, Áp Suất Chất Lưu, Phân Tích Độ Nhạy, Hiệu Suất Giếng Dầu

[1]*Khoa Địa Chất và Dầu Khí, Trường Đại học Bách Khoa TP.HCM, Việt Nam*

[2]*Đại học Quốc Gia Thành phố Hồ Chí Minh, Thành phố Hồ Chí Minh, Việt Nam*

[3]*Công ty điều hành khai thác dầu khí Cửu Long JOC, Việt Nam*

Liên hệ

Tạ Quốc Dũng, Khoa Địa Chất và Dầu Khí, Trường Đại học Bách Khoa TP.HCM, Việt Nam

Đại học Quốc Gia Thành phố Hồ Chí Minh, Thành phố Hồ Chí Minh, Việt Nam

Email: tqdung@hcmut.edu.vn

Lịch sử

- Ngày nhận: 17-5-2021
- Ngày chấp nhận: 27-9-2021
- Ngày đăng: 05-11-2021

DOI : 10.32508/stdjet.v4iSI3.847

Check for updates

VNU-HCM Press

Trích dẫn bài báo này: Thịnh N H, Dũng T Q, Hoanh P V. **Ảnh hưởng của nhiệt độ lên áp suất và lưu lượng dòng chảy trong giếng khai thác** . *Sci. Tech. Dev. J. - Eng. Tech.;* 4(SI3):1-1.